The Compton profiles of vanadium oxides

The Compton profiles of vanadium oxides

Chu-Nan Chang, Chuhn-Chuh Chen and Huey-Fen Liu

Department of Physics, National Taiwan Normal University, Taipei, Taiwan, Republic of China

Abstract. The isotropic Compton profiles of vanadium oxides VO, V_2O_3, VO_2, V_6O_{13}, and V_2O_5 were measured by using 59.54 keV γ-rays. The Compton profiles calculated by using the molecular-cluster model were found to be improper in describing the experimental results of VO and VO_2. The molecular-cluster model seems to underestimate the metal–ligand covalency. The localization and delocalization of valence electrons when forming oxides will be discussed on the basis of the atomic superposition model.

1. Introduction

Many compounds exist in the vanadium–oxygen system. A lot of experimental and theoretical studies [1–8] have been performed on the solid-state structures and other properties such as the metal–insulator transition. The crystal structures of many of these vanadium oxides have been determined, but the results of band-structure calculation varied in different approaches and were applied in different fields. Compton profiles may provide a direct check on the band calculations [9,10]. Unfortunately, up to now there have not been many such Compton profile calculations to be found in the literature. Recently, Gupta and Ellis [2], using molecular-cluster approximations, made the first isotropic and directional Compton profile calculation for VO and VO_2. This prompted us to conduct the isotropic Compton profile measurements for VO, V_2O_3, VO_2, V_6O_{13} and V_2O_5. These measurements have revealed some interesting features in the Compton profiles, and which are qualitatively related to changes in the wavefunctions of valence electrons, especially vanadium d electrons in the various vanadium oxides.

2. The experiment

2.1. The set-up

An annular source of about 1 Ci of Am^{241} was used for a 59.54 γ-ray backscattering measurement. The scattering angle was geometrically calculated to be 174°. Both the target and the radioactive source of Am^{241} were housed in a vacuum chamber at a pressure of less than 10^{-5} mb. The backscattering γ-rays passing through a beryllium window holding the vacuum were detected by a HpGe low-energy detector (ORTEC-GLP-16195-10) whose resolution was estimated to be 324 eV at the Compton peak of

48.3 keV. This resolution is extrapolated from the resolution of 400 eV at 59.54 keV by the scaling law $\Delta E \propto \sqrt{E}$. The overall momentum resolution of this experimental set-up is therefore about 0.50 au.

The powders of vanadium oxides with purity greater than 99.5% were pressed into disks 2.0 mm thick and 14 mm in diameter. In making the targets of the relatively unstable chemicals of VO, V_2O_3, and VO_2, special care was taken to preserve their chemical stoichiometries. The thickness and weight of each target were measured before and after the experiment. No significant change in these quantities was observed.

The Compton backscattering spectrum was automatically recorded every 30 minutes by a personal-computer-controlled MCA and the spectral line of the 5.9 keV x-rays of Fe[55] source was used to check the system stability. The drift of the Compton peak is estimated as less than 0.5 channel. In this experiment, each channel is equal to 32 eV.

2.2. The data reduction

The final result of the Compton profile was deduced from the raw spectrum by following a series of corrections. After the background was subtracted, the target self-absorption correction was followed by the method described elsewhere [11]. The detector efficiency was reconfirmed experimentally to be the same in the energy region of 30–60 keV.

· The correction for the 59.54 keV elastic escape peak due to the escape of the germanium K x-rays from the detector was made by using a collimated 10 mCi source of Am[241] put at the target position, even though its contribution to the Compton spectrum is less than 0.1%.

The spectrum so obtained showed no observable asymmetry about the Compton peak within about 40 channels, and therefore no corrections that might come from source self-scattering [12] and the non-Gaussian tail of the detector's response function were made.

Since the low-energy part of the spectrum was uncertain for the reason mentioned above, we have therefore analysed the high-energy part of the spectrum to obtain the Compton profiles. For the purpose of experimentally checking our measuring system and the data reduction procedure, we have also made a Compton profile measurement of vanadium powder in this work.

The instrumentation function, consisting of both the angular dispersions of incident as well as the back-scattering beams and the detector's resolution function, has been approximated as a Gaussian with FWHM = 325 eV. A Fourier-transform method was employed to do the deconvolution [13, 14], and a soft cut-off method [15] was utilized to eliminate the noise amplification included in the high-frequency region. The soft cut-off parameters κ and λ in equation (7) of [15]

$$F(\nu) = [1 + \lambda(2\pi\nu)^\kappa / G^2(\nu)]^{-1} H'(\nu)/G(\nu) \tag{2.1}$$

were determined via a chi-square fitting process. For example, $\kappa = 3$ and $\lambda = 10^{-4}$ were found for vanadium. The corresponding residual instrumentation function is listed in table 1 along with the vanadium Compton profile. The deconvolution spectrum was corrected for second multiple-scattering effects which had been calculated by the Monte-Carlo method. This Monte-Carlo calculation method was suggested by Felsteiner *et al* [16] and demonstrated by Pikanen *et al*

[17]. In this work, we have also experimentally investigated the influence of the second multiple-scattering effect, by studying V_2O_5 samples with thickness of 2, 4 and 8 mm (with identical densities). The results have confirmed the Monte-Carlo calculations. The third multiple scattering was found to be insignificant and was therefore simply neglected.

The double differential cross section so obtained was converted into a Compton profile $J(P_z)$ by use of the formula derived from the relativistic impulse approximation theory [18, 19]:

$$J(P_z) = [1/C(\omega_2, \omega_1, \theta, P_z)] \, d\sigma/d\Omega \, d\omega_2 \qquad (2.2)$$

in which ω_1, ω_2 are the frequencies of the incident and scattered photons, respectively; θ is the scattering angle and P_z is the electron momentum projected along the scattering vector, which can be expressed as

$$P_z = -[E_1(\omega_1 - \omega_2) - \hbar\omega_1\omega_2(1 - \cos\theta)]/c[\omega_1^2 + \omega_2^2 - 2\omega_1\omega_2\cos\theta]^{1/2} \qquad (2.3)$$

here E_1 is the electron energy which can be approximated by the rest-mass energy of the electron, $m_0 c^2$, without introducing a significant error. The factor $C(\omega_2, \omega_1, \theta, P_z)$ used here is the relativistic version for the scattering angle of 180° which also introduces a negligible error for our scattering angle of 174°.

The Compton profile of vanadium in this work is compared with those of Rollason *et al* [20] in table 1. These two sets of data (normalized to the same area of 10.31 for 0–7 au) are in good agreement within statistical errors. The data of Rollason were directional ones. The data of Rollason for the [100], [110] and [111] directions have been averaged via Houston's method [21] to obtain the isotropic Compton profile. The Compton profiles of vanadium oxides with the core contribution subtracted are listed in tables 1 and 2. The normalization areas for all these compounds are also shown in parentheses in these tables.

3. Results and discussion

All the results shown in tables 1 and 2 are the Compton profiles of the valence electrons, in which the core electrons of vanadium and oxygen have been subtracted. Statistical errors are shown at some data points. The corresponding theoretical values have been convoluted by our residual instrumentation function (RIF). For VO and VO_2, both the molecular-cluster model (MO) calculations [2] and the atomic superposition model (AS) results are listed for comparisons. In the MO model, a potential constructed from Hartree–Fock–Slater neutral atomic charge density was used, and the covalent mixing between the oxygen 2p and the vanadium 3d was seen to be somewhat larger in VO_2 than in VO. In the AS model, the atomic Compton profiles calculated by Biggs *et al* [22] for neutral atoms were used, and the Compton profile of each vanadium oxide was simply the superposition of the atomic profile of vanadium with the appropriate chemical valence (V^{2+} for VO and V^{4+} for VO_2, etc) and the atomic profile of oxygen $2p^6$. Both of them are scaled from the results of Biggs *et al* [22]. For example, the electron configuration used in the AS the Compton profile of VO is $V(3d^3 4s^0) + O(2p^6)$ and that of VO_2 is $V(3d^1 4s^0) + 2O(2p^6)$. Since V_6O_{13} is a mixed-valence oxide consisting of a

Table 1. The Compton profiles of metallic vanadium, VO and V_2O_3. The statistical errors for all the experimental data are shown for some data points. The number quoted in parentheses for each substance is the normalization area in 0–7 au. Note that only the Compton profiles of valence electrons for VO and VO_2 are shown here. All theoretical values (MO stands for molecular cluster approximation and AS stands for atomic superposition model) have been convoluted by the residual instrumentation function (RIF) which is shown in the fourth column.

Substances	Metallic vanadium (10.31)			VO (14.27)			V_2O_3 (32.46)	
P_z (au)	Exp.	Rollason	RIF	Exp.	MO	AS	Exp.	AS
0	5.21±0.03	5.21±0.03	6.64	2.87±0.04	2.65	2.75	6.94±0.11	7.08
0.1	5.20	5.19	6.48	2.85	2.65	2.75	6.92	7.07
0.2	5.13	5.13	6.05	2.85	2.66	2.75	6.95	7.08
0.3	5.02	5.04	5.44	2.82	2.63	2.74	6.94	7.03
0.4	4.87	4.89	4.79	2.77	2.61	2.71	6.89	6.93
0.5	4.69	4.71	4.23	2.71	2.56	2.65	6.79	6.76
0.6	4.48	4.50	3.82	2.63	2.50	2.57	6.63	6.54
0.7	4.24	4.27	3.56	2.52	2.42	2.46	6.38	6.21
0.8	3.99	4.02	3.42	2.39	2.31	2.32	6.05	5.83
1	3.47±0.03	3.51±0.02	3.23	2.06±0.03	2.03	2.00	5.21±0.10	4.94
1.2	2.99	3.01	2.93	1.69	1.74	1.67	4.27	4.06
1.4	2.57	2.57	2.56	1.32	1.46	1.36	3.31	3.26
1.6	2.20	2.21	2.21	1.00	1.22	1.10	2.51	2.59
1.8	1.89	1.87	1.92	0.78	1.00	0.89	1.90	2.05
2	1.66±0.02	1.63±0.01	1.66	0.63±0.02	0.80	0.71	1.48±0.06	1.62
3	0.94±0.01	0.91±0.01	0.92	0.27±0.01	0.29	0.25	0.56±0.04	0.53
4	0.64	0.63	0.64	0.11	0.04	0.10	0.22	0.21
5	0.47	0.48	0.48	0.05	0.03	0.05	0.11	0.11
6	0.35	0.36	0.37	0.02	0.03	0.04	0.03	0.07
7	0.27	0.27	0.28	0.01	0.03	0.03	0.03	0.06

Table 2. Same as in table 1 except for VO_2, V_6O_{13} and V_2O_5. The contributions of core electrons have also been subtracted.

Substances	VO_2 (18.19)			V_6O_{13} (113.0)		V_2O_5 (40.29)	
P_z (au)	Exp.	MO	AS	Exp.	AS	Exp.	AS
0	4.06±0.06	3.87	4.33	26.23±0.43	27.56	9.55±0.15	10.24
0.1	4.04	3.86	4.32	26.11	27.49	9.51	10.21
0.2	4.03	3.86	4.32	26.07	27.50	9.50	10.21
0.3	4.00	3.84	4.29	25.87	27.28	9.44	10.12
0.4	3.96	3.81	4.23	25.62	26.88	9.34	9.88
0.5	3.89	3.75	4.11	25.17	26.14	9.16	9.69
0.6	3.81	3.67	3.97	24.60	25.18	8.94	9.32
0.7	3.67	3.55	3.76	23.69	23.83	8.59	8.81
0.8	3.50	3.40	3.51	22.48	22.24	8.16	8.20
1	3.03±0.05	3.05	2.94	19.22±0.34	18.59	7.02±0.13	6.82
1.2	2.50	2.67	2.39	15.64	15.09	5.79	5.51
1.4	1.95	2.27	1.90	12.30	11.91	4.60	4.32
1.6	1.50	1.84	1.49	9.69	9.33	3.61	3.37
1.8	1.17	1.40	1.17	7.59	7.29	2.79	2.62
2	0.93±0.03	0.99	0.91	5.84±0.21	5.66	2.13±0.08	2.02
3	0.35±0.02	0.35	0.28	2.04±0.16	1.74	0.75±0.06	0.60
4	0.15	0.13	0.11	0.67	0.67	0.30	0.23
5	0.07	0.06	0.06	0.27	0.35	0.11	0.12
6	0.04	0.04	0.04	0.19	0.24	0.03	0.08
7	0.03	0.03	0.03	0.07	0.18	0.06	0.06

$4d^{4+}(d^1) + 2d^{5+}(d^0)$ electron configuration, its AS Compton profile is calculated from the configurations of $[4V(3d^14s^0) + 8O(2p^6)]+[2V(3d^04s^0) + 5O(2p^6)]$. Comparison with a free-ion superposition model would not be very useful, since the O^{2-} density depends strongly upon the external boundary condition imposed [23]. One must bear in mind that the metal–ligand covalency was not explicitly considered in the AS model.

In order to see more clearly the differences between theory and experiment, $\Delta J = J_{th} - J_{exp}$ is shown in figure 1. The disagreements between our data and the theoretical values are statistically significant. The experimental Compton profiles of VO and VO_2 are sharper than the MO calculations. Since sharper Compton profiles mean more extended wavefunctions, we thus suspect that the MO theory could underestimate the metal–ligand covalency which induces bonding charge distribution between atoms. The MO theory predicts stronger covalency in VO_2 than in VO and therefore, brings the theory closer to the experiment. However, one must note that the better agreement between the MO theory and the experimental results in VO_2 does not necessarily imply this since the MO calculation was performed for the high-temperature metal phase of VO_2 and our data were taken at room temperature (VO_2 is in the insulator phase).

The disagreements between the AS model calculation and the experiment as shown in figure 1 is to be expected since the vanadium oxides are not ionic binding substances, whereas the AS model, as stated above, is close to the ionic binding picture. However, the differences between the AS model and the experiment do provide some useful information about the electronic structures of these oxides. Examining figure 1, one immediately realizes that the wave functions of all valence electrons in VO should be more extended than they are in the form of ionic bondings. If this wave extension is due to the metal–ligand covalency induced by the hybridization of the oxygen 2p and the vanadium 3d orbitals as discussed on the basis of the molecular-cluster model, then the reverse trend predicted by the MO model deserves further investigation. On the contrary, the wavefunction predictions for the valence electrons in VO_2, V_6O_{13}, and V_2O_5 are too extended in the AS model and should be more localized.

We also list in table 3 the FWHM of the Compton profile for the experiment and the AS model, for comparison. The gradual decrease of the FWHM in the AS model for the higher oxidation state just reflects the fact that the charge transfer according to the chemical valence is higher. The differential of the FWHM between the experiment and the AS model again indicates the valence electrons are more extended in VO, and more localized in VO_2, V_6O_{13}, and V_2O_5 as compared to the respective 'ionic bonding' molecules.

Table 3. The linewidths (FWHM) of the Compton profiles for the vanadium oxides. Both values of the experiment and the AS model are shown.

Samples	VO	V_2O_3	VO_2	V_6O_{13}	V_2O_5
Exp.	2.68	2.73	2.74	2.70	2.74
AS	2.78	2.66	2.58	2.57	2.53

The experimental linewidth as well as the Compton profiles are bound to the exact electronic structures of vanadium oxides so they do not show any systematic change according to the oxidation states. Nevertheless, it is interesting to note that the experimental linewidth of VO_2 is the largest one among the oxides studied here
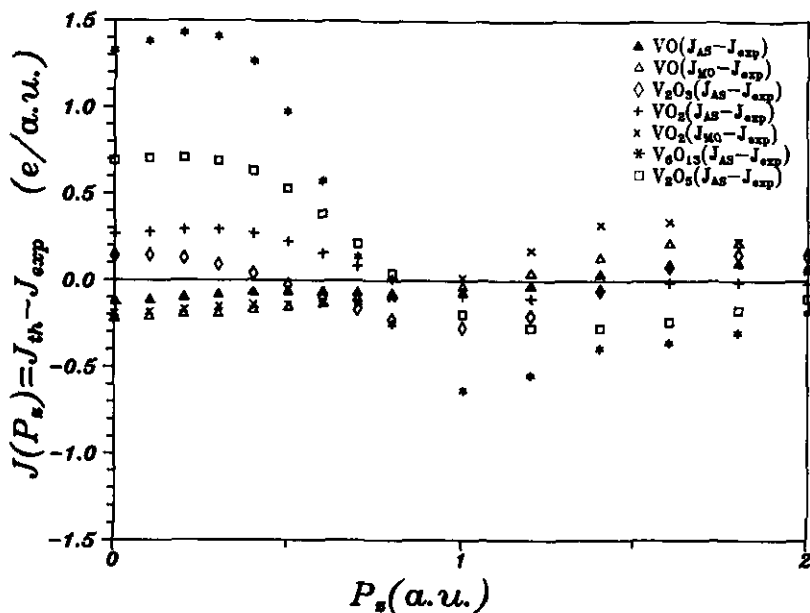
Figure 1. The difference between the theory and the experiment for the vanadium oxide Compton profiles. Note that the total number of electrons in each oxide is different.

and even larger than VO which chemically retains three 3d electrons around the vanadium ion whereas VO_2 retains only one. This may be partly due to the fact that VO_2 is an insulator at room temperature. V_2O_5 also has relatively large linewidth. The Compton profile study on the metal–insulator transition may be very interesting. Apparently, a deeper insight into the electronic structure of vanadium oxides rests on the theoretical Compton profile calculation of these oxides. Unfortunately, as far as we know, no such theoretical Compton profiles have been performed along this line except the aforementioned VO and VO_2 which are calculated within the framework of the molecular-orbital model.

4. Conclusion

In this work, we have presented isotropic Compton profiles for the vanadium oxides of VO, V_2O_3, VO_2, V_6O_{13}, and V_2O_5 at room temperature. We have shown that the Compton profiles calculated by the molecular-cluster approach (MO) for VO and VO_2 deviate substantially from our data. The metal–ligand covalency in the MO calculation may be underestimated. The variation of the experimental Compton profiles with respect to those of the atomic-superposition-model (AS) calculations for the vanadium oxides indicates that the valence electron wavefunctions, especially the vanadium 3d wavefunctions are more extended in VO, and more localized in VO_2, V_6O_{13}, and V_2O_5 than would be expected in the virtually 'ionic bonding' molecules of the respective vanadium oxides.

Acknowledgments

References

[1] Caruthers E, Kleinman L and Zhang H I 1973 *Phys. Rev.* B 7 3753
[2] Gupta M and Ellis D E 1976 *Phys. Rev.* B 13 3405
[3] Salem S I, Chang C N and Nash T J 1978 *Phys. Rev.* B 18 5168
[4] Shin S, Suga S, Taniguchi M, Fujisawa M, Kanzaki H, Fujimori A, Daimon H, Ueda Y, Kosuge K and Kachi S 1990 *Phys. Rev.* B 41 4993
[5] Abbate M, de Groot F M F, Fuggle J C, Ma Y J, Chen C T, Sette F, Fujimori A, Ueda Y and Kosuge K 1991 *Phys. Rev.* B 43 7263
[6] de Groot F M F, Grioni M, Fuggle C, Ghijsen J, Sawatzky G A and Petersen H 1989 *Phys. Rev.* B 40 5715
[7] Lambrecht W, Djafari-Rouhani B, Lannoo M and Vennik J 1980 *J. Phys. C: Solid State Phys.* 13 2485
[8] Fiermans L, Clauws P, Lambrecht W, Vandenbroucke L and Vennik J 1980 *Phys. Status Solidi a* 59 485
[9] Cooper M J 1985 *Rep. Prog. Phys.* 48 415
[10] Williams B G (ed) 1977 *Compton Scattering* (New York: McGraw Hill)
[11] Chang Chu-Nan, Lee Syh-Bin and Chen Chuhn-Chih 1991 *J. Phys. Soc. Japan* 60 4253
[12] Rollason A J, Felsteiner J, Bauer E W G and Schneider J R 1987 *Nucl. Instrum. Methods* 256 532
[13] Stokes A R 1948 *Proc. Phys. Soc.* 61 382
[14] Rollelt J S and Higgs L A 1962 *Proc. Phys. Soc.* 79 87
[15] Paatero P, Manninen S and Paakkari T 1974 *Phil. Mag.* 30 1281
[16] Felsteiner J, Pattison P and Cooper M 1974 *Phil. Mag.* 30 537
[17] Pikanen T, Laundy D, Holt R S and Cooper M J 1986 *Nucl. Instrum. Methods* 251 536
[18] Eisengerger P and Reed W A 1974 *Phys. Rev.* B 9 3237
[19] Ribberfors R 1975 *Phys. Rev.* B 12 2067
[20] Rollason A J, Holt R S and Cooper M J 1983 *Phil. Mag.* B 47 51
[21] Houston W V 1948 *Rev. Mod. Phys.* 20 161
[22] Biggs F, Mendelsohn L B and Mann J B 1975 *At. Data and Nucl. Tables* 16 201–309
[23] Fukamachi T and Hosoya S 1971 *J. Phys. Soc. Japan* 31 980